The Dynamic Behaviour of a Crystal During Defect Jumps

II. Self Correlations During Vacancy Jumps from an MD Simulation

R. Vogelsang and C. Hoheisel

Theoretische Chemie, Ruhr-Universität Bochum

Z. Naturforsch. **41 a,** 1051 – 1059 (1986); received May 7, 1986

In continuation of a previous paper, MD simulations of vacancy jump in an fcc-lattice have been performed. due to an increased averaging process, quantitative results for a number of correlation functions are obtained, which throw light on the details of the highly cooperative mechanism of vacancy jumps involving some fifty neighbouring particles. This Part II is mainly concerned with self correlation functions while part III focusses on distinct correlation functions. Both the mean square displacements and the velocity correlations of the particles have been considered and were analysed in comparison with those of a pure crystal and a pure fluid of high density.

1. Introduction

Molecular dynamics (MD) studies of the vacancy jump of an impurity atom in a Lennard-Jones crystal have been reported in a previous paper [1]. Unfortunately, most of the results in [1] could only qualitatively be interpreted due to the relatively low averaging level.

In this paper a vacancy jump not involving an impurity is studied. The averaging procedure has been enlarged to ensure that all of the presented time correlation functions are evaluated by averaging over at least 1000 events [2]. So the correlation functions became accurate to about 5 per cent. The present part II of our work concerns the autocorrelation functions, while in part III distinct correlation functions shall be discussed.

Our studies exploit the Bennett method [3] to model the jump process in a lattice. This method has a few disadvantages and might not simulate the jump process realistically with regard to all aspects [4]. However, the Bennett method can certainly serve as a means to understand the jump behaviour of real solids. We are here particularly interested in the short time behaviour of the particles involved rather than in transport coefficients which are essentially determined by the asymptotic long time behaviour [5].

The neighbourhood of the split vacancy is illustrated in Figure 1.

Reprint requests to Prof. Dr. C. Hoheisel, Theoretische Chemie, Ruhr-Universität Bochum, Universitätsstraße 150, D-4630 Bochum.

2. Method of Computation

The simulations have been performed with 256 argon like atoms including one jumping atom (see Table 1). Four essential improvements of the computations have been achieved:

(i) enhancement of the number of events for the evaluation of the correlation functions (CF) by about a factor of 100;

(ii) conservation of the total momentum of the crystal to 10^{-6};

(iii) conservation of the total energy of the system to 10^{-5};

(iv) suppression of any disturbing effects of the "restricted model potential" on the behaviour of the computed CFs.

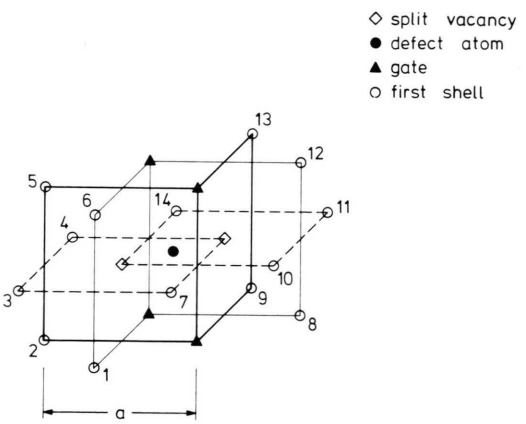

Fig. 1. Scheme of the lattice in the region of the split vacancy (see also Table 3). The lattice constant, a, amounts to 1.5859 σ.

0340-4811 / 86 / 0800-1051 $ 01.30/0. – Please order a reprint rather than making your own copy.

Table 1.

A) Technical details of the MD runs		
Number of particles (N)		$255+1$
Time step		0.5×10^{-14} s
Number of time steps		10^5
Cut off radius		$2.5\,\sigma$
CPU-time for 100 integration steps		2.2 s
B) Lennard-Jones (12–6) potentials		
Interaction	(ε/k_B)/K	σ/Å
Ar–Ar	119.8	3.405
Defect Ar–Ar (modified)	119.8	3.03

Table 2. Thermodynamic state of the model crystal.

Density	$\frac{N}{V}\sigma^3$	1.0028
Temperature	Tk_B/ε	0.51
Lattice parameter	a/σ	1.5859
Compressibility factor *		2.10
Potential energy *	$-u_{pot}/\varepsilon$	7.11

* uncorrected.

Table 3. Particle groups considered in this work.

Group	Number of particles	Characterization	Remarks
Defect atom	1	initially in an interstitial site near the centre of the lattice	saddle point configuration
Gate atoms	4	nearest neighbours of the defect atom in the interstitial site	smallest distances
1st shell atoms	14	nearest neighbours of the two vacancies	gate atoms excluded
2nd shell atoms	~ 35	next nearest neighbours of the defect atom in the interstitial site	gate atoms and 1st shell atoms excluded

Point (i) could be accomplished by an appropriate vectorization of the FORTRAN program, which allowed an acceleration of the simulation by about a factor 25 [2]. An additional reduction of the necessary computational effort has been obtained through a more effective generation of saddle-point configurations (see Appendix).

Point (ii) was essentially achieved by an alternate processing of the motion of the jumping particle during the reflections caused by the "restricted potential" (see Appendix).

Point (iii) has been fulfilled using the method of momentum dissipation described in the Appendix.

Point (iv) was ensured by a proper choice of the parameter R_x governing the "restricted potential". This choice was possible by means of a lot of extra runs with different potential parameters.

Our improved MD-simulation technique generated a very stable average temperature of the model lattice which had not to be corrected after about each 30th jump event as was necessary in [1].

3. Calculation of the Correlation Functions

All the CF's in the present work refer to restricted ensemble averages [6]. The dynamical variable probes only distinct local regions of the ensemble. Thus only subsets of particles can be used to form the average value. Improvement of the statistics is only possible by averaging over different time origins.

To get a low statistical error of about 5% for the mean square displacement (MSD) of the jumping particle, we have to average over more than 1000 trajectories of the jumping particle obtainable from different saddle point configurations. This requires about 100000 time steps for the simulation. In contrast, the evaluation of the MSD of a particle of a perfect Lennard-Jones (LJ) lattice requires only runs of 2000 steps, as each particle of the lattice can be chosen for the averaging. The MSD of a perfect lattice is thus accurate to 1–3%.

The thermodynamic state investigated here is specified in Table 2.

4. Particle Groups Considered

As in [1] we have considered the correlations of different groups of particles involved in the jump. This time, however, we have included a wider neighbourhood of the split vacancy. The characterization of these particle groups is given in Table 3.

The CF's of the more numerous particles of the larger neighbourhood are more accurate than those for the jumping atom or the gate atoms.

5. Results

5.1. Mean Square Displacements

5.1.0. Jumping Atom

Figure 2 displays the MSD of the jumping atom and that of an atom in the perfect crystal. The jumping atom reaches its stationary MSD much later than the perfect lattice atom. This indicates that the MD simulation for the perturbed lattice is reasonably performed, artificial effects being suppressed. We see that during the first 0.75 ps the MSD of the jumping atom increases strongly and reaches its near lattice position. The behaviour of the MSD resembles that of the reaction coordinate, ξ, defined in Section 2 of the Appendix and plotted in Figure 3. However, the short time form of these functions (0.5 ps) differs markedly. While the MSD of the jumping atom increases approximately quadratically with time, the reaction coordinate grows linearly. This is reasonable, since the reaction coordinate reflects the motion of the jumping atom as well as that of the gate atoms. Apparently for times smaller than 0.5 ps, ξ is primarily determined by the gate motion – of which the MSD is nearly linear in this time range (compare Fig. 4) – whereas for longer times it is predominantly governed by the motion of the jumping particle.

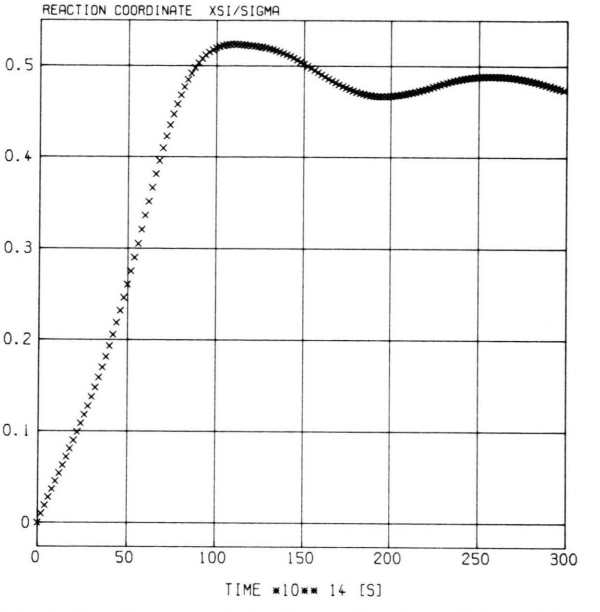

Fig. 3. Reaction coordinate, ξ, as a function of time. ξ in σ-units. Origin: saddle point configuration.

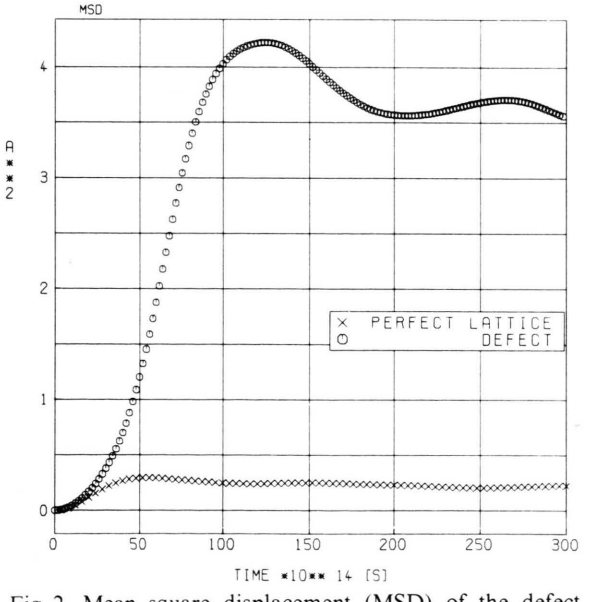

Fig. 2. Mean square displacement (MSD) of the defect atom during the jump compared with the MSD of perfect lattice atoms. Units: $Å^2$.

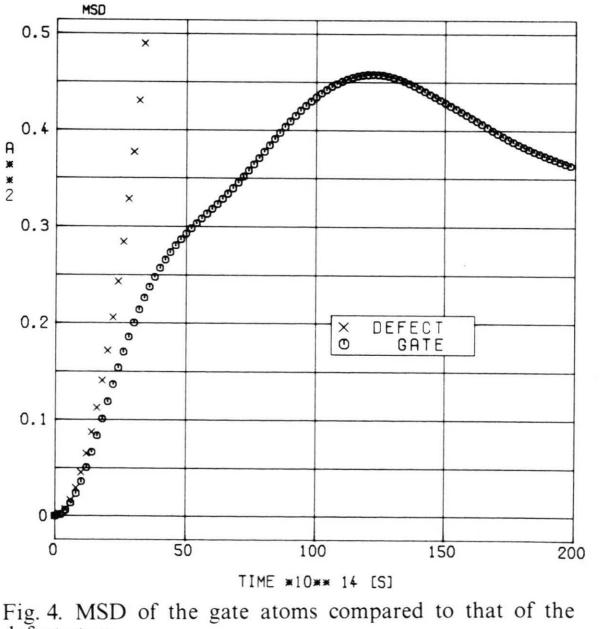

Fig. 4. MSD of the gate atoms compared to that of the defect atom.

5.1.1. Gate Atoms

The MSD of the four gate atoms is displayed in Fig. 4 together with that of the jumping atom. Interesting are the two slopes occurring during the increase of the gate MSD. The MSD of the gate atoms starts with a speed similar to that of the jumping atom. It shows a nearly linear behaviour in the time ranges 0–0.3 ps and 0.3–1.0 ps. The asymptotic value is reached after 2 ps. The slope of the MSD is flatter in the time region 0.3–1.0 ps than in the initial period, and the change of the slope concides reasonably with that of the reaction coordinate.

The MSD of the gate atoms illustrates most significantly the closing of the gate which apparently proceeds in two steps: initially, the gate atoms move very quickly to their equilibrium positions in agreement with the motion exhibited by a perfect lattice atom (compare Figure 2). After about 0.3 ps, however, their motion is hampered by the jumping atom, which has not yet left the range of the gate, as can be seen in Figs. 2 and 4. This short time behaviour of the gate resembles that of fluid particles under very high pressure and temperature, as shows the MSD of particles of a super-critical fluid studied in [7]. Figure 6 of that work shows a similar characteristic change of the slope of the MSD during the first 0.8 ps.

The "amplitude" of the MSD of the gate atoms is about a factor of 10 smaller than that of the jumping particle.

5.1.2. Atoms of the First and Second Shell (see Table 3)

Figure 5 shows the MSDs of the first and second shell atoms together with that of a perfect lattice atom. While the MSD of the second shell atoms is nearly equal to that of a perfect lattice atom, the first shell atoms reach a larger MSD, which decreases linearly in the range of 1–2 ps. So there exists a significant correlation between the motion of the defect atom, the gate atoms and the first shell atoms. On comparing the MSDs of the gate (Fig. 4), the first shell and the second shell atoms (Fig. 5), an increasing shift of the maxima of these MSDs is noticeable.

5.2. Velocity Autocorrelation Function

5.2.0. Jumping Atom

The velocity autocorrelation function (VACF) of a jumping atom for two averaging levels is shown in Figure 6. This figure illustrates the low statistical error of our correlation functions. As already men-

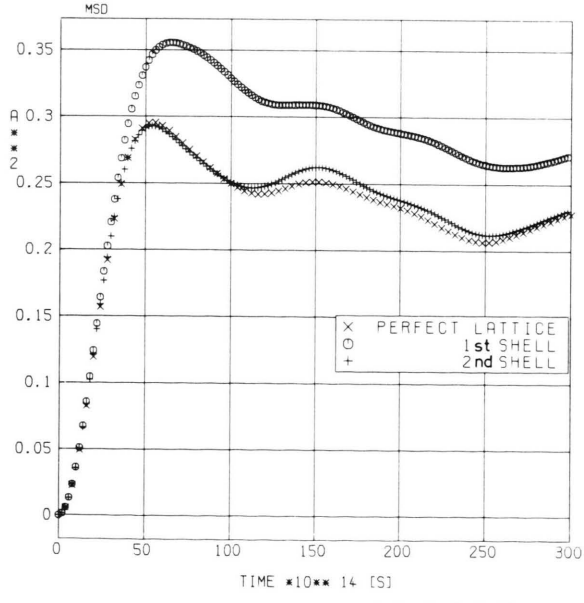

Fig. 5. MSD of the 1st-shell atoms and the 2nd-shall atoms compared with that of perfect lattice atoms.

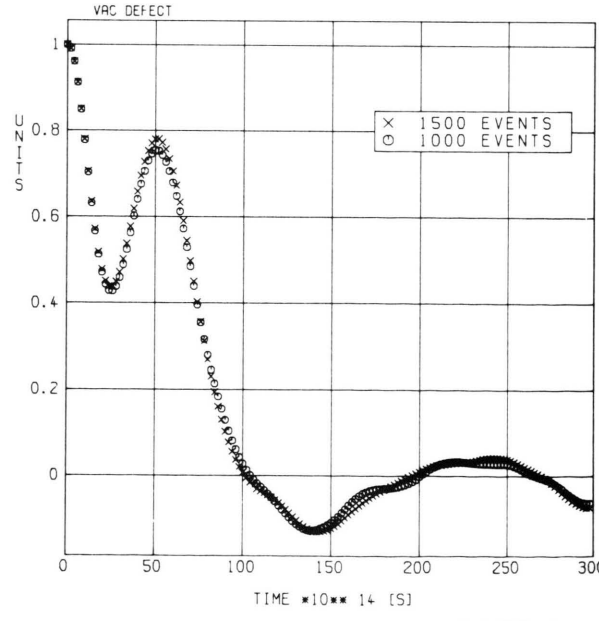

Fig. 6. Velocity autocorrelation function (VACF) (normalized) of the jumping atom for two averaging niveaus.

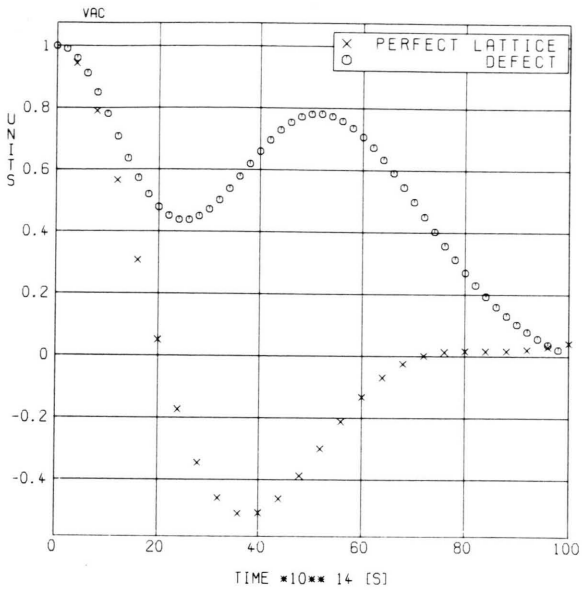

Fig. 7. VACF of the defect atom and perfect lattice atoms.

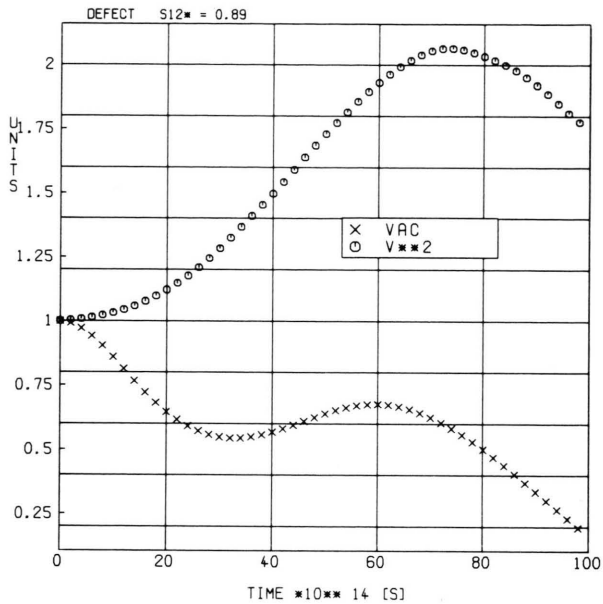

Fig. 8. VACF of the defect atom for a Lennard-Jones lattice of a reduced σ_{12} parameter of 3.031 Å (crosses). Autocorrelation function of the absolute amount of the velocity (V**2) of the defect particle (circles).

tioned, the correlation functions for the jumping atom have by far the largest statistical error.

The VACF shows an interesting intermediate minimum at about 0.25 ps. Figure 7 illustrates that such a minimum is not found for a perfect lattice atom. Initially both VACF's decay similarly, but after 0.1 ps the velocity decorrelation of the jumping atom is not continued. A focussing of the velocity of the jumping particle occurs, leading to an increase of the VACF in the range of 0.25–0.5 ps. After this period, the expected steady and relatively slow decorrelation process is noticeable ending after about 1 ps, where the particle has reached the vacancy position. An explanation for this remarkable short time behaviour of the jumping particle can be given in connection with the gate motion. Starting from the saddle point configuration gate and the jumping atoms perform at the beginning the common lattice vibrations, but immediately after this initial motion they tend to occupate their original places. During this latter period the gate begins to close and the jumping atom is thrown from its saddle point plateau in direction to the vacancy site. Therefore the velocity of the defect atom is focussed and accordingly the VACF passes the observed intermediate maximum. At the same time, the MSD of the gate atoms changes its slope, as we have discussed in paragraph 5.1.1. Furthermore the intermediate maximum of the jumping particles VACF is in accordance with the behaviour of the reaction coordinate showing two different slopes during that time.

We have studied this intermediate increase of the VACF in more detail in terms of the ACF of the absolute amount of the jumping particle velocity and by changing the σ_{12} parameter governing "spatial" interactions between the jumping atom and the host atoms (see Table 1 B). The results are plotted in the next Figure 8. We see that the ACF of the absolute amount of the velocity increases steadily in the time range discussed above. Apparently the jumping atom is accelerated steadily when it starts from the saddle point plateau. This confirms our considerations on the focussing effect of the closing gate atoms on the jumping particle.

The second correlation function shown in Fig. 8 (crosses) is the VACF of the defect atom for the case of a reduced σ_{12} Lennard-Jones potential parameter. Compared to that displayed in Fig. 7 the intermediate maximum is here much lower indicating that the motion of the gate influences the defect atom motion essentially less due to the weaker coupling; so this finding agrees well with our results discussed above.

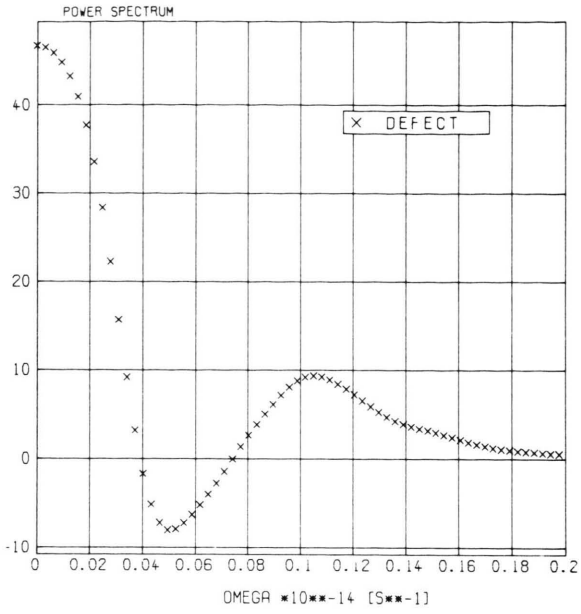

Fig. 9. Power spectrum of the VACF of the defect atom.

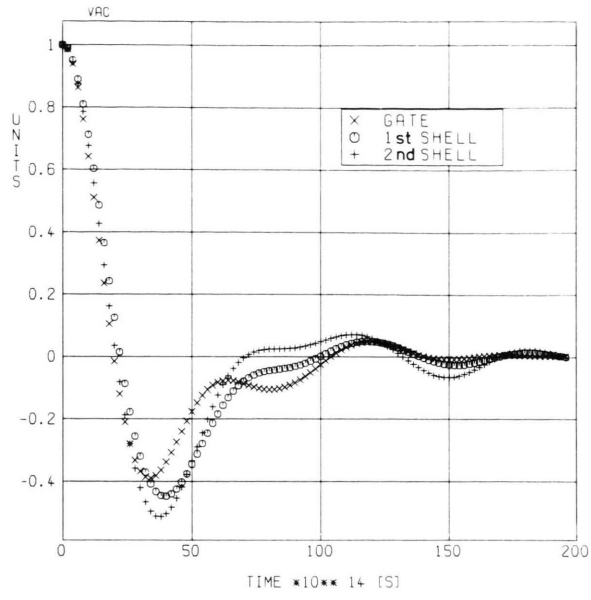

Fig. 10. VACF of the gate, the 1st-shell and the 2nd-shell atoms.

Apparently a strong increase of the correlation occurs after 0.25 ps, when the gate is closing and the defect particle is thrown in direction of the vacancy. We shall discuss this point in detail in paper III, where the distinct correlations are considered.

According to the intermediate increase of the VACF of the defect particle, the power spectrum (one-sided cosine transform), which is plotted in Fig. 9 shows a very uncommon form. Diffusive and oscillatory modes are mixed and the interpretation seems to be difficult.

5.2.1. Gate Atoms

In Fig. 10, we have plotted the VACF of the gate atoms, the first and second shell particles.

As expected, the gate VACF departs appreciably from the others and resembles that of a fluid particle at high pressure (compare Fig. 7 of [7]). The first minimum of the gate VACF is less deep than that of the other particles and a maximum follows. This confirmes completely what we have already stated in 5.1.1: due to the initial closing phase of the gate the decorrelation of the momentum arises more rapidly than that of the other particles. The "backscattering" is however smaller in amplitude, since appreciable momentum and energy are transferred to the jumping atom (inducing effect), but it is more extended in time, as the transfer goes periodically.

Furthermore, comparing Fig. 10 and 6, we find immediately that the first minimum of the defect particle VACF corresponds in time to the first turning point of the gate VACF (zero crossing), and the first maximum coincides with the second turning point (end phase of the "backscattering" process). These observation lend support to our model of the induced momentum transfer between gate and defect particle.

In Fig. 11 we compare the spectrum of the gate particle VACF with that of a perfect argon crystal. There is a noticeable deviation between the first main peaks at low frequency (transversal modes). The peak is smaller for the gate particles and has a sharp top at lower frequency. The side peaks at higher frequency (longitudinal modes) agree however essentially. Such a decrease of the intensity of the higher frequency transversal eigenmodes might be understandable because the momentum transfer between gate particles and jumping atom occurs dominantly via modes of higher frequency. More details could be obtained by analyzing the wave vector dependent current-current CF. However, this analysis would exceed the frame of the present study.

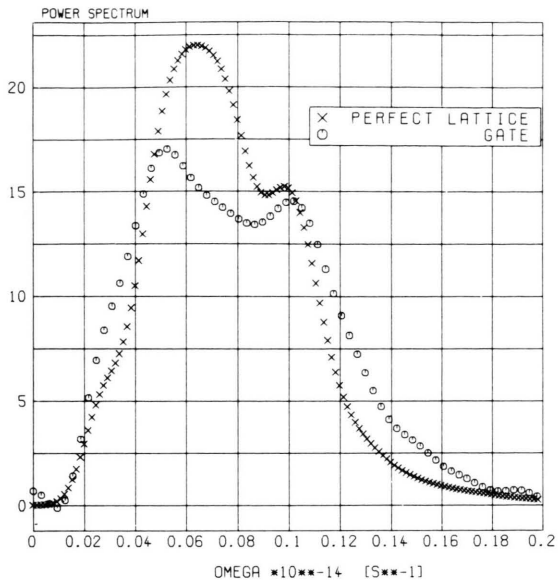

Fig. 11. Power spectrum of the gate VACF in comparison with that of a perfect lattice.

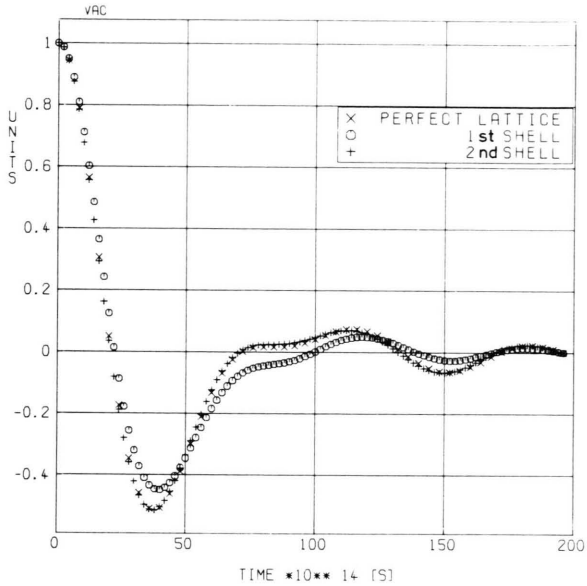

Fig. 12. As in Fig. 10, but for the 1st-shell and the 2nd-shell atoms compared with a particle of a perfect lattice.

5.2.2. First and Second Shell Atoms

A comparison of the VACF of the first shell and second shell atoms with that of an undisturbed lattice atom is made in terms of the plots shown in Figure 12. Evidently, the VACF of the second shell atoms does not deviate from the VACF of the normal argon lattice. This confirms our statement given in paragraph 4.

We see furthermore that the first shell atoms participate noticeably in the jump process. The smaller minimum of the VACF and the extended "backscattering" period indicate a closing of these particles similar to that of the gate atoms, however, phase shifted and to a much weaker extend, as we shall see in the next report.

The power spectrum of the VACF of these first shell atoms does not differ markedly from that of a normal lattice atom. It shows a more damped structure, but permits otherwise no detailed interpretation.

6. Discussion and Conclusions

In terms of the mean square displacement and the autocorrelation function of four groups of particles involved in the jump process, we have analyzed the dynamic behaviour of an argon like crystal during vacancy jumps. We have used the Bennett method for our investigation, as this is a suitable means to study such a process. The main results are:

(i) The duration of the jump process is similar to that of a lattice vibration;
(ii) the short time behaviour of the jumping atom is decisively determined by the closing motion of the gate atoms (zero time corresponds to saddle point configuration);
(iii) closing of the gate atoms has a "focussing" effect on the velocity of the jumping atom;
(iv) first shell atoms participate significantly in the jump process and perform a gate like closing motion, however much more weakly;
(v) second shell atoms show no coupling to the jump process. Their space and momentum behaviour is not correlated with that of the three other particle groups (see Table 3).

As far as our present model calculations indicate, the gate atoms play the central role for the jump process. They induce the motion of the jumping atom on one hand and retard the "closing motion" of the first shell atoms on the other hand. The retardation is well illustrated by the plot of the VACFs shown in Figure 10. While the strongly

decaying branch of the VACFs falls in line for the gate and the second shell atoms, it is significantly shifted to larger time for the first shell atoms.

A final point of interest is the marked decay of the jumping atom VACF. Apparently the jumping atom moves here like an unperturbed lattice atom. So the saddle point configuration represents a dynamical plateau area for the interstitial particle which is not well comparable with a sharp top of an energy barrier [4, 5]. The jumping particle stays about 0.2 ps in this area which corresponds to 20 per cent of the total jump period. Our consecuting report on the distinct correlations will throw more light on this.

Appendix

1. Modelling of a Jump of a Defect Atom in a Lattice

Consider an fcc-lattice with a defect atom D, which implies a vacancy site (VS) in the neighbourhood of D. During a jump, D has to pass from its equilibrium position (EP) through the gate of four atoms (GA) to the VS leaving a vacancy site at its former position. In other words, on its path D has to cross an energy barrier formed by the four GA. The configuration, where D has arrived at the plateau of the barrier is called saddle point configuration (SPC). Near the melting point, D possesses sufficient kinetic energy to cross the gate frequently so to allow investigation of the jump process with reliable statistics by standard computer simulations [8]. Computer simulations are also directly useable for the investigation of fast ionic conductors like CaF_2, where the F-ions show a liquid like diffusion [9, 10].

Apart from these special cases, the jumping frequencies of impurity atoms are usually very low in crystalline solids compared with the time scale of molecular dynamics simulations (MD). Therefore, no jump-event would be observable within an MD run of reasonable length. Due to this, one has to enhance the jump frequency artificially to model the jump behaviour of a crystal by MD. This method of inducing successful trajectories was first suggested by Bennett [3] to investigate diffusion in solids.

2. The Method of Induced Trajectories

The method is based on a restricted potential:

$$u^*(r_1 \dots r_N) = u_{\mathrm{LJ}}(r_1 \dots r_N) + u_{\mathrm{D}}(\xi) + u_{\mathrm{WS}}$$

with

$$u_{\mathrm{D}} = \begin{cases} 0 & |\xi| < R_x, \\ \infty & |\xi| \geqq R_x, \end{cases}$$

u_{WS}: single occupancy term keeping atoms other than D within its Wigner-Seitz cell.

ξ is the reaction coordinate of the jumping atom given in terms of the four gate atoms 1, ..., 4:

$$\xi = [\boldsymbol{r}_{\mathrm{D}} - \tfrac{1}{4}(\boldsymbol{r}_1 + \boldsymbol{r}_2 + \boldsymbol{r}_3 + \boldsymbol{r}_4)]\, \boldsymbol{j},$$

where $\boldsymbol{j}$ is a unit vector in jump direction, chosen to be in the (110) direction.

R_x is an arbitrary upper bound value for $|\xi|$.

> u^* restricts the system to a region of phase space which intersects all successful jump trajectories between the two lattice sites in question, except for a few unsuccessful trajectories. That means, in terms of u_{D} the jump atom is reflected by an infinite potential wall whenever $|\xi| \geqq R_x$.

A reflection is roughly an inversion of the velocity $\boldsymbol{v}_{\mathrm{D}}$. This momentum inversion is to be dissipated by the lattice, otherwise the total momentum ($\boldsymbol{p} = 0$) and the energy are not conserved.

Due to our choice of ξ, the four gate atoms have to be involved in the momentum dissipation. We achieved this in a similar way known from the collision of hard spheres.

At time $t = t_0$ assume

$$\xi(t = t_0) \geqq R_x .$$

Then calculate

$$\boldsymbol{R}'_{\mathrm{D}}(t) = \boldsymbol{R}_{\mathrm{D}}(t) - \Delta\boldsymbol{R}(t),$$
$$\boldsymbol{R}'_i(t) = \boldsymbol{R}_i(t) - \Delta\boldsymbol{R}_i(t), \quad i = 1,$$

and

$$\Delta\boldsymbol{R}_{\mathrm{D}i} = \Delta\boldsymbol{R}_{\mathrm{D}} - \Delta\boldsymbol{R}_i .$$

Project $\Delta\boldsymbol{R}_{\mathrm{D}i}$ onto the jump direction:

$$\boldsymbol{j}' = \boldsymbol{j} \cdot F \quad \text{with} \quad F = \begin{cases} +1 & \xi > 0 \\ -1 & \xi < 0 \end{cases},$$

$$\Delta\boldsymbol{R}'_{\mathrm{D}i} = -(\Delta\boldsymbol{R}_{\mathrm{D}i} \cdot \boldsymbol{j}')\, \boldsymbol{j}'$$

and recalculate $\Delta \boldsymbol{R}_D$ and $\Delta \boldsymbol{R}_i$

$$\Delta \boldsymbol{R}'_D = \Delta \boldsymbol{R}_D + \Delta \boldsymbol{R}'_{Di},$$

$$\Delta \boldsymbol{R}'_i = \Delta \boldsymbol{R}_i - \Delta \boldsymbol{R}'_{Di}.$$

With $\Delta \boldsymbol{R}'_D$ and $\Delta \boldsymbol{R}'_i$ one obtains the new coordinates of $\boldsymbol{R}_D$ and $\boldsymbol{R}_i$

$$\boldsymbol{R}''_D = \boldsymbol{R}'_D + \Delta \boldsymbol{R}'_D,$$

$$\boldsymbol{R}''_i = \boldsymbol{R}'_i + \Delta \boldsymbol{R}'_i.$$

On the other hand, for $\xi(t = t_0) < R_x$ one has to check whether ξ has changed its sign with respect to $\xi(t = t_1)$.

A change of the sign indicates a saddle point configuration. This configuration is then stored.

The decision whether the jump is successful or not is made in an MD run described in Section 3.

For computational purposes, we used a cube of edge d_{WS} of half the lattice constant rather than a Wigner-Seitz dodecahedron. Whenever the separation between an atom j and its ideal lattice site is larger than $d_{WS}/2$, the atom is displaced back by $\Delta r_j(t)$.

The potential term u_{WS} is only necessary for calculations near the melting line.

3. Details of the Simulation

The simulation of the hopping process consists of four MD-runs:

run 1

Thermalize an fcc-lattice with D on a normal lattice site. Store the coordinates of the ideal lattice sites and the deviations of the last configuration with respect to the ideal lattice.

run 2

Start from the thermalized ideal lattice configuration, search for the centre particle and exchange its coordinates with those of D. Remove one particle from the nearest neighbourhood of D to obtain a certain jump direction (here (110)). After positioning D in a SPC ($\xi = 0$), all the neighbours of D in a certain range are marked.

Choose a reasonable value for R_x. Due to some geometrical considerations one finds that $|\xi|$ could reach a maximum value of about 0.5σ. Therefore a value of $R_x = 1.0\sigma$ ensures that u_D has no direct influence on D.

Add the coordinate deviations to retain the configuration of run 1 and thermalize this configuration again. The last configuration is stored with D set into the saddle point.

run 3

Start from the last configuration of run 2 with R_x: $0.1\sigma - 0.2\sigma$. Store a certain number of SPC during this run.

run 4

Use the SPCs collected in run 3 to compute exact trajectories for a chosen time interval by common MD.

During this run the correlation functions described in the text are evaluated according to the list of group of particles made in run 2.

Pursuing each trajectory one is able to decide whether D reaches the new vacancy or falls back into its old position. A jump is regarded as a successful one only when the sign of ξ remains unchanged and a final value of $\xi = 0.5$ is reached.

Acknowledgements

We are grateful to Prof. A. Klemm for critical comments and helping to clarify the presentation of the report. – We thank D. Haake (for photographs), S. Peterhansl (for typing), the "Rechenzentrum der Ruhr-University Bochum" (for computations on the CYBER 205) and the "Deutsche Forschungsgemeinschaft" (for financial support: Ho 626/6-1, Ho 626/6-2).

[1] K. D. Becker and C. Hoheisel, J. Chem. Phys. **77,** 5108 (1982).
[2] R. Vogelsang, M. Schoen, and C. Hoheisel, Comp. Phys. Commun. **30,** 235 (1983); M. Schoen and C. Hoheisel, Molec. Phys. **52,** 33 (1984).
[3] C. H. Bennett, in: Diffusion in Solids (A. S. Nowick and J. J. Burton, ed.), Academic Press, London 1975.
[4] G. Jacucci, in: Diffusion in Crystalline Solids (G. E. Murch and A. S. Nowick, eds.), Academic Press, London 1984.
[5] M. Toller, G. Jacucci, G. De Lorenzi, and C. P. Flynn, Phys. Rev. B **32,** 2082 (1985).
[6] C. Hoheisel and M. D. Zeidler, Molec. Phys. **54,** 1275 (1985).
[7] R. Vogelsang and C. Hoheisel, Molec. Phys. **53,** 1355 (1984).
[8] D. R. Squire and W. G. Hoover, J. Chem. Phys. **50,** 701 (1969).
[9] G. Jacucci and A. Rahman, J. Chem. Phys. **69,** 4117 (1978).
[10] A. Rahman, J. Chem. Phys. **65,** 4845 (1976).